

# Numerical Modelling final project

Vincent Mokuenko

March 4, 2024

## 1 Introduction

The Agulhas Current is the western boundary current of the South Indian Ocean anti-cyclonic gyre. It is known as the primary current of the Southern hemisphere with large surface velocities (above  $1 \text{ m.s}^{-1}$ ) and volume transport (between 60 and 150  $\text{Sv}$  [2]). Located at the limit between two large basins, the Agulhas system plays a major role in the interchange of water masses between the southern Indian and the southern Atlantic oceans. The Agulhas flows from the Mozambique channel, southward, following the African coast, until meeting the Agulhas bank and changing direction southward. It is in this region that we find the strongest current. Contrary to other western boundary current, meanders are not frequently observed in this region. When the current leaves the continental shelf and flows as an inertial jet, mesoscale become numerous. The southern part of our domain (described below), is the region where the current retroflects before flowing eastward, back toward the Southern Indian ocean. The retroflection is associated with shedding of warm eddies that transport water northwestward. The purpose of this project is to perform a numerical simulation of the Southern Agulhas current and its retroflection, using atmospheric forcing and a realistic map of the topography. We use the Coastal and Regional Ocean COmmunity model (CROCO) in a regional configuration. We will analyse the outcome of the model to estimate if it can accurately reproduce the key features in the region. First, we will briefly describe the setup of the simulation and then present the main results with a qualitative comparison with observations and/or simulations from the literature.

## 2 Numerical Simulation

The simulation is a run of the CROCO model in a realistic configuration. We choose to represent the region of the Agulhas system. The main point of interest of this region is the retroflection of the Agulhas current and the associated events of shedding of warm-core rings into the South Atlantic. To properly visualize these events, we choose a domain extending meridionally from  $5^\circ$  to  $30^\circ\text{E}$  and zonally from  $30^\circ$  to  $45^\circ\text{S}$  with a horizontal resolution of  $1/8^\circ$  and 32 vertical levels. Our domain consists of a horizontal grid of  $154 \times 201$  points. The simulation is set to last 2 years and is forced using climatological data sets for atmospheric forcing and topography. Accordingly, the domain's boundaries are opened, allowing exchanges and variations in the total energy. The outcome of the first year will not be shown, as it serves as a spin up time for the system to represent accurately the response to atmospheric forcing. We will thus refer to the beginning of the second year as the initial time  $t = 0$ . The spatial resolution of the domain serves as a constraint for

the barotropic and the baroclinic timesteps of the simulation according to

$$\Delta t_{bc} \leq \frac{0.843686}{c_1 \sqrt{\frac{1}{\Delta x^2} + \frac{1}{\Delta y^2}}}, \quad \Delta t_{bt} \leq \frac{0.89}{\sqrt{gH \left( \frac{1}{\Delta x^2} + \frac{1}{\Delta y^2} \right)}} \quad (1)$$

where  $H \approx 5000$  m is the maximum depth in the domain and  $c_1$  is the phase speed of the fastest internal waves, we choose a large value for  $c_1 \approx 8 \text{ m.s}^{-1}$ . Using the mean spatial resolution  $\Delta x \sim 12.04$  km and  $\Delta y \sim 12.02$  km, we obtain a maximum baroclinic timestep  $\Delta t_{bc} \sim 900$  s and barotropic timestep  $\Delta t_{bt} \sim 34$  s. Our simulation uses a margin for the baroclinic timestep, and we choose  $\Delta t_{bc} = 850$  s with 35 barotropic iterations between each baroclinic timestep.

### 3 Results

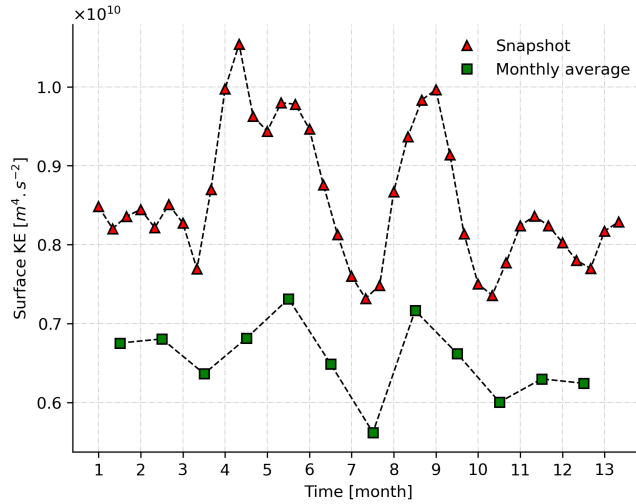


**Fig. 1:** Time evolution of the surface kinetic energy for the monthly averaged velocity (green squares) and for every 10 days snapshots (red triangles).

#### Total kinetic energy

The temporal evolution of the kinetic integrated over the domain shows strong seasonal variability (**Fig.1**). We observe two major peaks around the 4th and 9th months which correspond to an increase of about 20% in the total surface kinetic energy compared to the mean value  $\overline{EK} = 8.6 \cdot 10^9 \text{ m}^4 \cdot \text{s}^{-2}$ . We also note a minimum around month 7/8 with a value of  $7.3 \cdot 10^9 \text{ m}^4 \cdot \text{s}^{-2}$ . The total surface kinetic energy is also shown for the monthly averaged output of the simulation (**Fig.1**). We observe a lower mean value (24 % decrease compared to the energy computed from 10 days snapshots) with similar tendencies for the extrema. This difference in the kinetic energy may be an indication of an intense small scale activity in the domain. Mesoscale/submesoscale processes that happen on a timescale shorter than a month may be filtered out, resulting in a lowered total energy. Strong seasonal variations may be the result of the different forcing that constrain the simulation such as wind stress, heat fluxes and short-wave radiations.

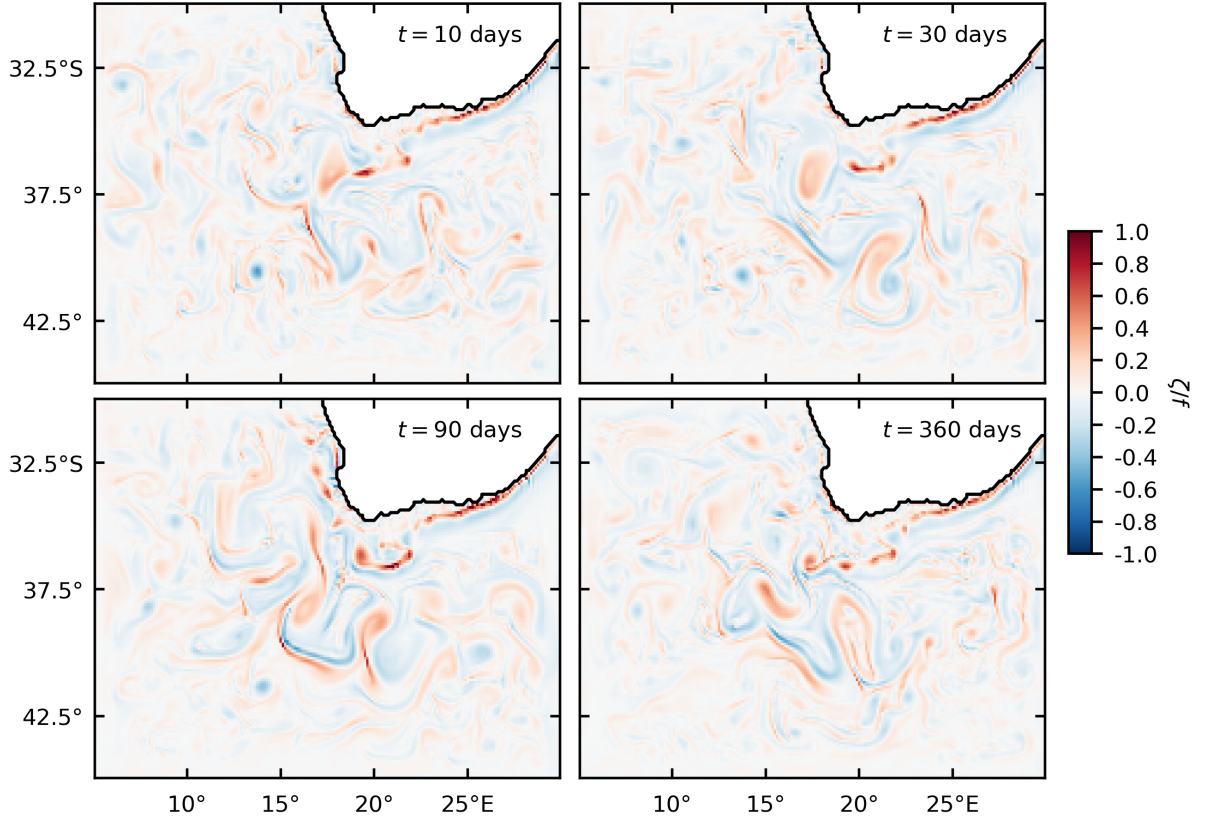


**Fig. 2:** Relative vorticity normalized by the local Coriolis parameter  $\zeta/f$  at the surface for  $t = 10, 30, 90, 360$  days.

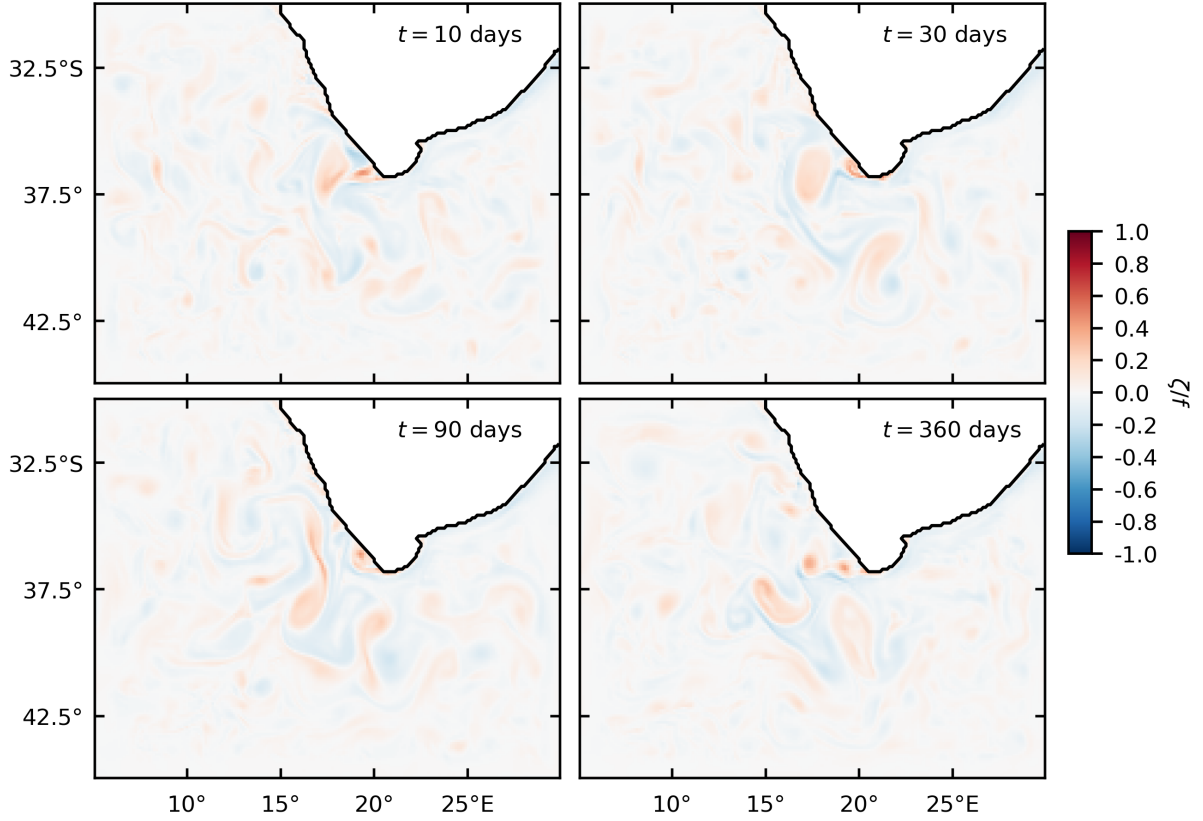


**Fig. 3:** Relative vorticity normalized by the local Coriolis parameter  $\zeta/f$  at 400 m depth for  $t = 10, 30, 90, 360$  days.

## Vorticity field

At the surface, we observe vorticity structures at different scales (**Fig.2**). In the region where the Agulhas Current flows southeastward (around 25°E, 35°S), it follows the South African coast and the frictional boundary layer generates cyclonic vorticity. When the current detaches from the coast, this results in intense cyclones drifting westward (shear-edge cyclones [?]). This is where the most intense values of vorticity are found at the surface. On the other side the current is also horizontally shear, creating a filament of negative vorticity. Those two structures interact when the current changes direction around 20°E, and the small cyclonic structures on the eastern edge of the Agulhas Bank (shear-edge eddies [3]) are surrounded by a layer of negative vorticity. Larger structures are created when the current turns southward after leaving the Agulhas bank, around 17°E. In the vicinity of the South African coast, we observe creation of very small patterns of cyclonic eddies, along the Agulhas bank, and flowing northward, following the continental shelf and the coast. Those structures drift northwestward and interact in a complex mesoscale field. We can observe vortex merging and filamentation of vorticity. At the South of the Agulhas Current (south of 42°S), we note a much weaker vorticity field, associated with a smaller spatial scale. The intensity of the vorticity field is also weaker in the eastern, and western parts of the domain. In the vorticity field at 400 m depth, we observe a similar behaviour as at the surface, with lowered intensity (**Fig.3**). The large surface structures are still present at -400 m (e.g. at  $t = 360$  days, around 20 °E, 40°S, we recover the same cyclonic structure that is present at the surface), with similar shapes. Although we observe variability in the kinetic energy, the vorticity field seems to be qualitatively invariant over the span of a year (not shown here). At every time during the simulation, we observe

shedding of large cyclones and anticyclones that drift northwestward, and are deformed in a complex turbulent field. Those coherent structures remain the largest over the year, and seem to extend at several hundred meters deep, with decreasing intensity.

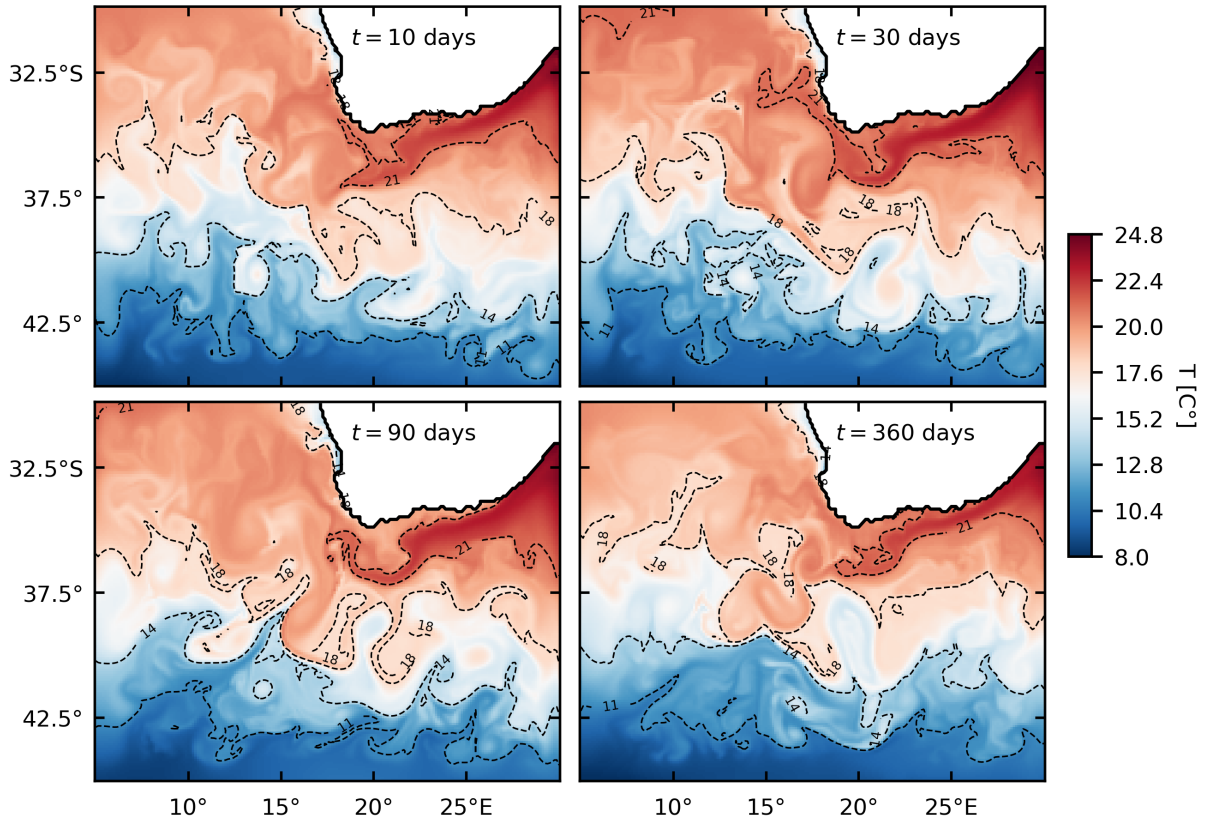


**Fig. 4:** Potential temperature at the surface for  $t = 10, 30, 90, 360$  days.

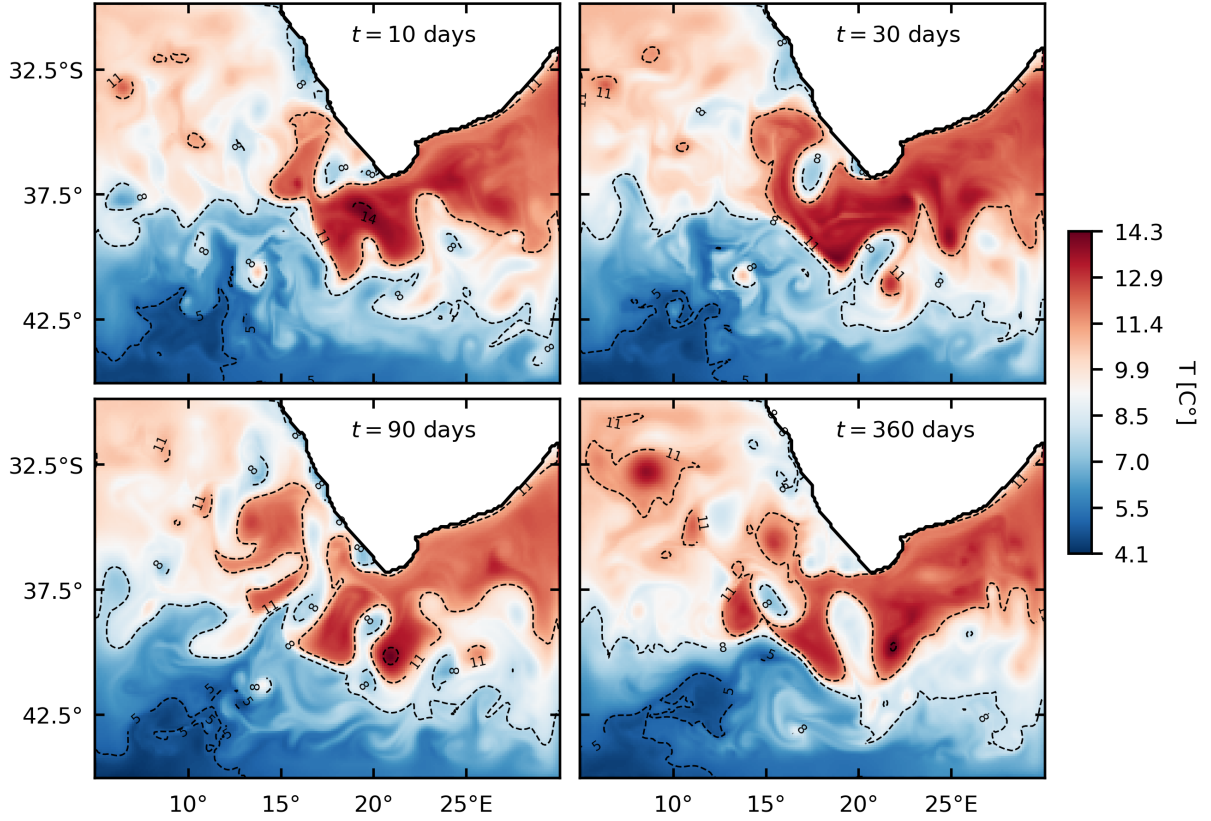
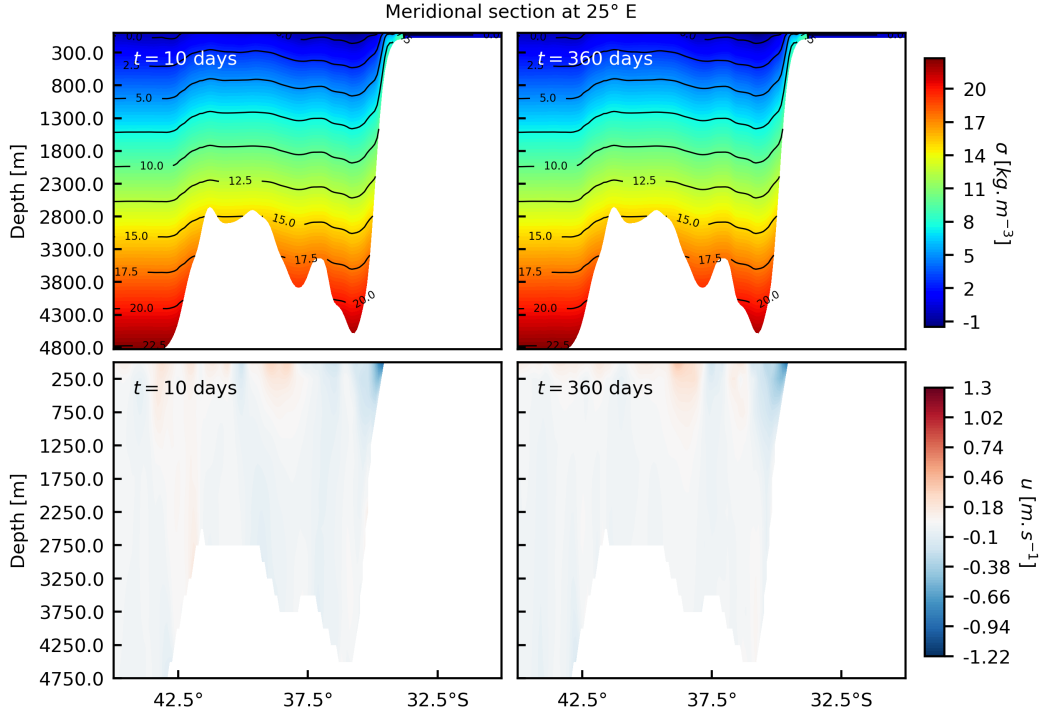


Fig. 5: Potential temperature at 400 m depth for  $t = 10, 30, 90, 360$  days.

## Potential temperature

Maps of potential temperature at different depths exhibit shedding of warm and cold rings, happening along the retroflection of the Agulhas current, when warm water coming from the Indian Ocean encounters cold water coming from southern regions. The potential temperature field in the domain is shown for both the surface and 400 m depth (Fig.4, Fig.5). We observe similar pattern in both cases. At first order, we observe warm water from the Indian Ocean that is brought in the region by the strong Agulhas Current from the North East. This is easily seen at the surface, we can observe thin band of temperature close to  $22^{\circ}\text{C}$ . This feature remains similar at 400m, although the temperature is lower. The advection of warm water is contrasted by the presence of much colder water at the South. This corresponds to water masses transported by the Circumpolar Current with a temperature around  $8^{\circ}\text{C}$  at the surface and  $5^{\circ}\text{C}$  at 400m. Those two water masses meet in the region of the Agulhas retroflection, and a resulting very strong temperature gradient is visible in this zone, especially at 400m (e.g. at 30 days, near  $18^{\circ}\text{E}$ ,  $39^{\circ}\text{S}$ ). Patches of high temperature seem to follow to advection of large vorticity structures northwestward. We observe the detachment of warm-core rings at different times. These rings are diffused while drifting northwestward, and the warm ring are getting colder as the structure are transported. When a ring is detached, we note a tongue of cold temperature extending northward. This results in smaller structures of cold temperature drifting similarly to the warm-core rings, at smaller scale. We observe respectively warm and cold rings at 400m, with a temperature of more than  $11^{\circ}\text{C}$  and less than  $8^{\circ}\text{C}$ , drifting northwestward at a similar pace. The resolution of the simulation allows to observe other processes such as coastal upwelling. Both temperature fields show a zone of colder temperature in the northern part of the domain, along the African coast ( $17^{\circ}\text{E}$ ,  $32^{\circ}\text{S}$ , with a temperature around  $18^{\circ}\text{C}$  at

the surface and around  $8^{\circ}\text{C}$  at  $-400\text{m}$ ). This patch may correspond to a region of coastal upwelling, induced by the wind forcing and the resulting Ekman transport, in the Benguela region.



**Fig. 6:** Meridional section of potential density anomaly  $\sigma$  (upper panel) and zonal velocity  $u$  (lower panel) for  $t = 10$  days (left panel) and  $t = 360$  days (right panel), at longitude  $15^{\circ}$  E.

## Density and velocity section

The meridional density section at  $25^{\circ}\text{E}$  shows potential density anomaly values  $\sigma$  between  $-1$  and  $23 \text{ kg.m}^{-3}$ , with isopycnals that tend to be fairly horizontal except in the vicinity of strong topographic features (Fig.6). Isopycnals are horizontal in the southern part of the domain, and between  $40^{\circ}\text{S}$  and  $35^{\circ}\text{S}$ , namely above the Agulhas plateau peaking at  $-2500\text{m}$ . We observe strong slopes in isopycnals surface in two distinct regions : (1) near the South African coast and (2) at the northern limit of the Agulhas plateau. Those two regions correspond to the Agulhas current flowing southwestward (1) and return current flowing back westward, after the retroflection (2). We note consistency in this observation with the zonal velocity section. The model seems to represent good agreement with thermal wind balance, strong density gradients can be related to zonal velocity. At  $35^{\circ}\text{S}$ , we find the highest values in zonal velocity, where the Agulhas Current flows at speed up to  $1 \text{ m.s}^{-1}$  and faster at the surface. This is associated with denser water in the shallow region and very strong isopycnal slopes. This current seems to extend over the entire water column at this latitude, although we observe decreasing velocity with depth. We observe surface velocity for the Agulhas Return Current of about  $0.8 \text{ m.s}^{-1}$  at a latitude of  $38.5^{\circ}\text{S}$ . Near the surface, we observe two light water anomalies on either sides of the Agulhas plateau. These anomalies may be linked to the advection of warm water from the Indian Ocean by the very strong surface current. We note the presence of eddies (recognized by alternating zonal velocity signs) with coherent velocity structure that extend down to  $2000 \text{ m}$ . Those eddies have surface velocity up to  $\sim 0.5 \text{ m.s}^{-1}$ . The densest water is found in southern

regions at the bottom of the water column, around 5000 m depth, with a density anomaly of  $22.5 \text{ kg.m}^{-3}$ .

## Mean velocity, surface displacement and eddy kinetic energy

The model seems to be able to reproduce accurate representation of the velocity in the region of the Agulhas retroflection. We observe strong surface current flowing with the Agulhas Bank on its right, with a surface velocities up to  $1.15 \text{ m.s}^{-1}$ . This result seems consistent with observations, thermal infrared satellite observations have shown a clear narrow and almost linear current [4]. The current loops anticlockwise after reaching the southern tip of the African Coast (around  $18^\circ\text{E}$ ) and we see evidence of the Agulhas Return Current, meandering in the region near the Agulhas Plateau ( $25^\circ\text{E}$ ). The mean velocity of the Return Current is not as high as that of the Agulhas Current, we observe mean surface velocities close to  $0.6 \text{ m.s}^{-1}$ . A maximum in velocity norm of  $0.6 \text{ m.s}^{-1}$  also occurs in the region where we observed strong temperature gradients ( $17^\circ\text{E}$   $40^\circ\text{S}$  visible in **Fig.4** and **Fig.5**). The region can be split into two distincts zones : the Northern and Southern parts. In the Northern part, we observe low mesoscale activity and very strong mean current. The kinetic energy is mostly dominated by the mean kinetic energy, this is where we note the highest velocity. This is consistent with previous observations, it has been shown that in this region, mesoscale activity is associated with occasionnal solitary meanders ("Natal Pulses" [3]) and shear-edge eddies in the vicinity of the Agulhas Bank. In the Southern part, we note maxima in both eddy kinetic energy and variance in the sea surface height, in the region where we could previously observe detachments of large eddies. We note localized values of EKE up to  $0.15 \text{ m}^2.\text{s}^{-2}$ , and a larger zone starting from the detachment of the current from the Agulhas Bank. In this region, hydrodynamical instabilities (mixed barotropic-baroclinic [6]), complex interactions with topography, and non-linear interactions between eddies and eddies/mean current explain this large value in EKE. We obtain qualitatively similar pattern in surface EKE as altimetric data (AVISO and ECCO2) and higher resolution CROCO simulation [6] [7] (standard deviation of SSH close to  $0.4 \text{ m}$ ), although our result seems less intense than observations. Maximum of SSH occurs around  $21^\circ\text{E}$   $39^\circ\text{S}$ , we obtain highest values close to  $0.1 \text{ m}^2$ , giving a maximum standard deviation of  $0.3 \text{ m}$ . Similarly to what we obtain for the EKE, we recover a maximum in SSH Standard deviation/variance near  $20^\circ\text{E}$  but observations from altimetry (TOPEX/POSEIDON) have shown significantly greater values close to  $0.4 \text{ m}$  [1].



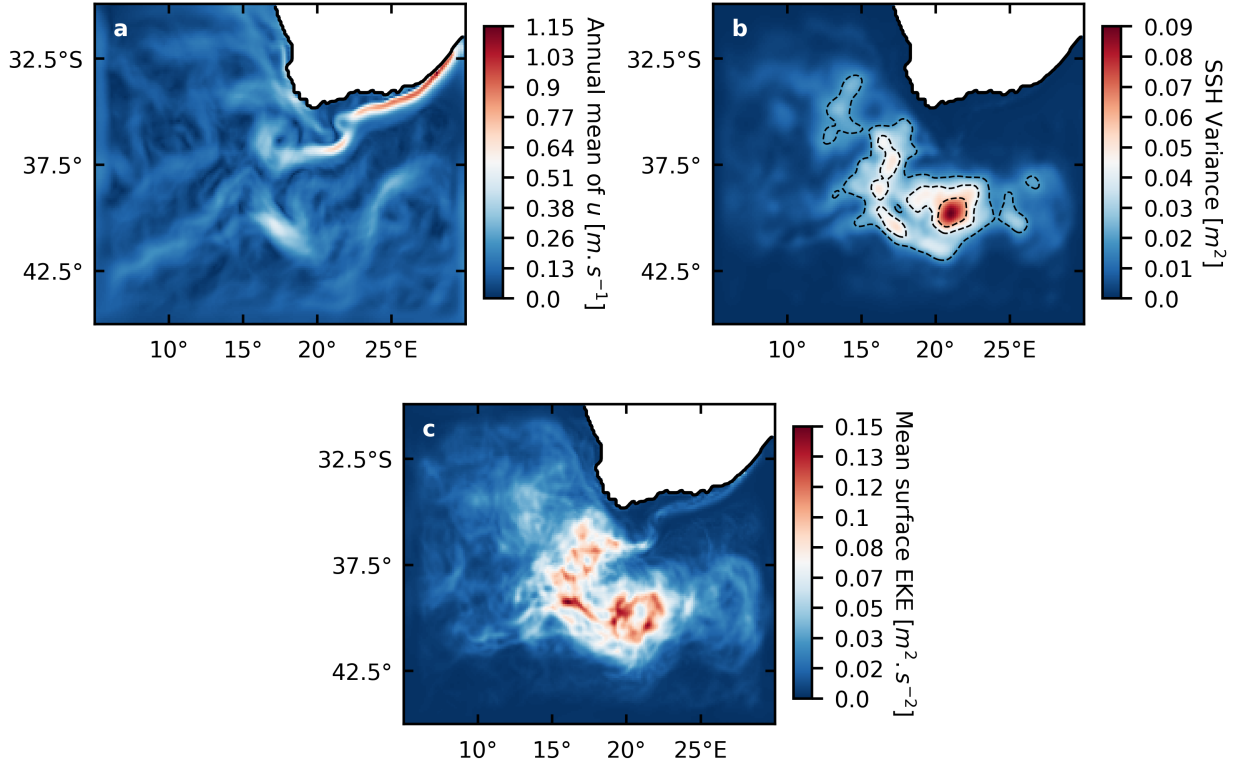


**Fig. 7:** **a.** Annual mean of the norm of the surface velocity  $U$ , **b.** variance of sea surface height  $\eta$ , **c.** mean surface eddy kinetic energy (EKE)

## Conclusion

Our simulation in the realistic CROCO configuration produces qualitatively accurate results. We recover the most important features in the region, well known from satellite or in situ observations and reproduced in larger numerical simulations. In our configuration the Agulhas current follows a well defined trajectory along the African coast in the Northern part, until detaching from the Agulhas bank and becoming an inertial jet, subject to instabilities. On the northeastern part of the domain, the Agulhas current seems to extend over the entire water column, decaying with depth. We observe the retroflection of the current, creating large warm rings, most easily seen in potential temperature maps at 400m depth. Shedding of eddies generates lots of variability in the trajectory of the mean current, and the kinetic energy in the southern region is dominated by EKE. This is consistent with results in sea surface anomalies. Additionally, the model seems to agree with observations in the northern region, where the eddy field is not as intense, and the current is thin and consistent, with very high surface velocity. This simulation produced qualitatively accurate results, showing that the Agulhas current can be simulated convincingly using atmospheric forcing and accurate topography of the region, although we find values in SSH variance and EKE that seem lower than observations. Simulations with larger spin up time, with a longer timespan or larger resolution, could be done to investigate the origin of this disagreement.

## References

- [1] W. P. M. DE RUIJTER, A. BIASTOCH, S. S. DRIJFHOUT, J. R. E. LUTJEHARMS, R. P. MATANO, T. PICHEVIN, P. J. VAN LEEUWEN, AND W. WEIJER, *Indian-atlantic interocean exchange: Dynamics, estimation and impact*, Journal of Geophysical Research: Oceans, 104 (1999), p. 20885–20910.
- [2] J. LUTJEHARMS, *The Agulhas Current*, Springer Berlin Heidelberg, 2006.
- [3] J. LUTJEHARMS, O. BOEBEL, AND H. ROSSBY, *Agulhas cyclones*, Deep Sea Research Part II: Topical Studies in Oceanography, 50 (2003), p. 13–34.
- [4] J. R. E. LUTJEHARMS, *Three decades of research on the greater agulhas current*, Ocean Science, 3 (2007), p. 129–147.
- [5] R. P. MATANO, C. G. SIMIONATO, W. P. DE RUIJTER, P. J. VAN LEEUWEN, P. T. STRUB, D. B. CHELTON, AND M. G. SCHLAX, *Seasonal variability in the agulhas retroflection region*, Geophysical Research Letters, 25 (1998), p. 4361–4364.
- [6] P. TEDESCO, J. GULA, P. PENVEN, AND C. MÉNESGUEN, *Mesoscale eddy kinetic energy budgets and transfers between vertical modes in the agulhas current*, Journal of Physical Oceanography, 52 (2022), p. 677–704.
- [7] Y. ZHU, B. QIU, X. LIN, AND F. WANG, *Interannual eddy kinetic energy modulations in the agulhas return current*, Journal of Geophysical Research: Oceans, 123 (2018), p. 6449–6462.